

ANALYSIS TECHNIQUES FOR THE PREDICTION OF SPRINGBACK
IN FORMED AND BONDED COMPOSITE COMPONENTS

53-24

51325

P-21

Michael F. Gasick
Senior Engineer
McDonnell Aircraft Company
St. Louis, Missouri

Dr. Gary D. Renieri
Senior Technical Specialist
McDonnell Aircraft Company
St. Louis, Missouri

SUMMARY

Two finite element analysis codes are used to model the effects of cooling on the dimensional stability of formed and bonded composite parts. The two analysis routines, one h-version and one p-version, are compared for modeling time, analysis execution time, and exactness of solution as compared to actual test results. A recommended procedure for predicting temperature effects on composite parts is presented, based on the results of this study.

INTRODUCTION

McDonnell Aircraft Company is actively involved in the research and development of advanced composite structures. The goals of lighter weight, lower cost, and more survivable composite aircraft structures are being pursued by several research projects. Innovative designs are being studied in conjunction with emerging materials to realize these goals.

Several studies utilizing the thermoplastic composite material system are currently in progress. Design, manufacturing, and testing of sub-scale and full-scale components are part of the research activities. An interesting phenomenon which has arisen during fabrication and bonding is a dimensional warpage or "springback" of the sub and full scale thermoplastic components. This warpage is caused by the difference in the coefficients of thermal expansion (CTE) in the principal directions of the

thermoplastic material. As the part is cooled, the difference in the in-plane and through thickness CTE's causes a build-up of thermal stresses. The residual thermal stresses cause a warpage when the part is removed from the tool. In some instances, the part deflected off the tool at the edges as it was cooled. The resultant springback can occur in thermoplastic, thermoset, or any other composite material with different directional CTE's.

Related investigations have been completed to attempt to predict the amount of springback in formed or bonded composite parts. Material properties have been shown to be important in the prediction of springback magnitudes, references [1] and [2]. The through thickness coefficient of thermal expansion is an influential material property. Fahmy and Ragai-Ellozy derived a formula to estimate the through thickness CTE in reference [3]. The formula is based on known in-plane thermal properties.

Finite element solutions have been used to predict springback for simple geometries with some apparent success, references [4]-[6]. The majority of work has demonstrated that simple geometries can be modeled for springback with a reasonable degree of accuracy. However, more complex shapes are much more difficult to model.

Additional work is being completed in research activities at McDonnell Aircraft Company. The degree of springback has been shown to be linked to the build-up of residual thermal stresses. The effects of tooling temperature and ply orientation on the magnitude of these residual stresses are being investigated. The residual stresses have been shown to dramatically affect the interlaminar tensile strength of thermoplastic test specimens.

PROBLEM STATEMENT

The need exists to develop a reliable technique to predict springback in formed and bonded composite structures. Current procedures for springback compensation involve the reworking of

tools after the magnitude of springback is observed on a final part. This operation is costly and must often be repeated several times, depending on the complexity of the part. Tooling can be designed to compensate for springback if a reliable analysis method can be formulated. The compensated tool would then be capable of producing parts which are dimensionally correct the first time and eliminate the need for rework.

The use of finite element methods to predict springback has shown promise. H-version finite element codes have been used to model simple geometries with reasonable agreement with actual data. Lesser degrees of accuracy and reliability are realized for more complex geometries. The p-version finite element approach is an alternative to the current h-version methods. The p-version formulation increases the degree of polynomial shape function for each element as the mesh is refined. The number of elements remains constant and, therefore, requires less modeling time than an h-version analysis. Thus far, however, very little work has been done using p-version finite element codes to predict springback magnitudes.

This paper compares the h and p-version finite element codes for predicting springback magnitudes. Simple and complex geometries of isotropic and orthotropic material properties are modeled. The two analytical methods are then compared for modeling time, analysis execution time, and exactness of solution as compared to actual test results.

DESCRIPTION OF ANALYSIS CODES

The two finite element codes chosen for comparison are COSTAR (h-version) and MSC/PROBE (p-version).

COSTAR, the COmposite STructural Analysis Routine, was developed by Jon Goering of the Structural Research Department of McDonnell Aircraft Company and is widely used in Research and Development projects. COSTAR elements are assembled and formulated

in a method similar to MSC/NASTRAN. Beam, shell, plate, and solid elements are available in linear, quadratic, and cubic forms. COSTAR is particularly well suited for the analysis of composite structures. The program has the ability to consider laminated and fully three-dimensional reinforced composites, as well as isotropic and orthotropic materials, reference [7]. The majority of figures in this paper were generated by the COSTAR post-processor.

MSC/PROBE uses the p-version approach to the finite element solution by increasing the degree of polynomial shape function of the element to the point of solution convergence. This feature often decreases modeling and solution time due to the requirement of fewer elements.

MSC/PROBE offers an error estimation routine in which the finite element solution is compared to the exact problem solution. The exact solution is based on the Principle of Virtual Work and is of the form;

(1)

in which δU is a bilinear expression for the virtual work of internal stresses and δW is a linear functional of the virtual work of external forces. Error estimation is based on solving the equation such that the difference between the finite element solution and the exact solution, based on the Principle of Virtual Work, is minimized. This can be expressed as;

(2)

in which u is the exact solution of Equation (1) and u_h is the user defined finite element solution. An excellent source of information on the formulations and methodology used in MSC/PROBE can be found in reference [8].

Other features such as the ability to calculate stress intensity factors around singularity points are available. The

author would refer readers to the MSC/PROBE User's Manual for detailed descriptions of other capabilities, reference [9].

BASELINE COMPARISONS

CASE I: SIMPLE GEOMETRY - ISOTROPIC MATERIAL

The initial test of the ability of COSTAR and MSC/PROBE to model springback was a simple isotropic hat section, Figure 1. The material properties used are as follows:

$$\begin{aligned} E &= 0.5 \times 10^6 \text{ psi} & \text{NU} &= 0.35 \\ \text{CTE} &= 0.31 \times 10^{-6} \text{ 1/}^\circ\text{F} \end{aligned}$$

The model discretization required for the two programs can be seen in Figures 2a and 2b. The COSTAR model required 388 elements and 980 degrees of freedom while the MSC/PROBE model required 32 elements and 1048 degrees of freedom at a p-level of 5. The applied load was a -500°F temperature gradient to represent the cooldown of the part from consolidation temperature. The constrained model is shown in Figure 1. These load and constraint conditions were used on all models for the duration of the study.

The displacement results for the simple geometry, isotropic case can be seen in Table 1. As can be seen, COSTAR and MSC/PROBE give the same displacement results for this configuration. The error estimation for MSC/PROBE p-levels 1-8 is seen in Table 2. The execution time for the two analyses is very similar for the single COSTAR run and the MSC/PROBE run for $p = 5$ only. The final deflected geometry can be seen in Figure 3.

CASE II: SIMPLE GEOMETRY - ORTHOTROPIC MATERIAL

The effect of material property on the results of the two analysis programs was then studied. The isotropic material of Case

I was changed to the following orthotropic properties:

$$\begin{array}{ll} E_{11} = 2.24 \times 10^7 \text{ psi} & \nu_{12} = 0.35 \\ E_{22} = 1.30 \times 10^6 \text{ psi} & \nu_{23} = 0.48 \\ E_{33} = 1.30 \times 10^6 \text{ psi} & \nu_{31} = 0.02 \end{array}$$

$$\begin{array}{ll} \text{CTE}_{11} = 0.10 \times 10^{-6} \text{ } 1/^{\circ}\text{F} & G = 0.79 \times 10^6 \text{ psi} \\ \text{CTE}_{22} = 0.165 \times 10^{-4} \text{ } 1/^{\circ}\text{F} & \\ \text{CTE}_{33} = 0.175 \times 10^{-4} \text{ } 1/^{\circ}\text{F} & \end{array}$$

All other model parameters were identical to Case I. The results again show very close agreement between the two models, Table 3. Error estimations for the Case II model are similar to the Case I calculations seen in Table 2. The deflected geometry can be seen Figure 4.

CASE III: REFINED MESH - ORTHOTROPIC MATERIAL

The effect of mesh discretization on the results of the MSC/PROBE model was demonstrated by performing an h-p extension at the two radii. The number of elements was increased to 40 which can be seen in Figure 5. The results of this analysis again show close agreement between the two programs. Table 4 shows the displacements calculated from this analysis which are nearly identical to the results of Case II, Table 3. The effect of the h-p extension on the energy norm error can be seen in Table 5. The calculated error between the exact solution and finite element solution is decreased for the same p-levels of Table 2.

CASES I - III RESULTS SUMMARY

The results of Cases I - III show nearly exact agreement between COSTAR and MSC/PROBE in the calculation of temperature induced displacements. Analysis execution times between a single COSTAR run and an MSC/PROBE p-level 5 run are similar. MSC/PROBE

provides an error estimation function which can be used to evaluate the accuracy of the MSC/PROBE model. An h-p extension on the MSC/PROBE model was shown to decrease the percent error in the energy norm for the simple hat geometry.

STIFFENED SKIN ANALYSIS

The results of the previous case studies indicate that COSTAR and MSC/PROBE will predict similar springback magnitudes for a simple geometry. The current research problem, however, is the springback encountered in the bonding of a thermoplastic hat-stiffened skin. This more complex geometry is modeled in an attempt to accurately predict the expected amount of springback.

Material properties for the corrugated panel and the flat skin panel to be bonded were determined using the program THICKLAM, reference 10. THICKLAM utilizes Classical Lamination Theory to derive three-dimensional elastic constants of composite laminates using the formulae of Jones and Sun, references 11 and 12. The three-dimensional properties are necessary due to the cross sectional geometry of the model. The model X axis follows a material 90° ply and the model Y axis is through the thickness of the skin. Therefore E1 of the model is Ey of the material and E2 of the model is Ez of the material, Figure 6. The material properties used for the corrugation and flat skin panels are shown in Tables 6a and 6b.

The COSTAR and MSC/PROBE finite element models are shown in Figures 7a and 7b. The COSTAR model required approximately 1500 elements and 2325 degrees of freedom while the MSC/PROBE model required 153 elements and 3400 degrees of freedom for $p = 4$. The material properties of Table 6 were used for the corresponding parts of the model and the proper local material properties were input into the MSC/PROBE model. The applied load was a -500°F temperature gradient as in the previous case studies. The constraints are again similar to the previous studies and are shown in Figure 6.

The results of this study again show close agreement between the two finite element programs, even for the more complex geometry. Table 7 shows the deflections for the two models. Figure 8 shows the deflected geometry of the COSTAR model which is essentially the same as the MSC/PROBE model. The more sophisticated model produced a greater error as can be seen in the calculations of Table 8. The COSTAR model required approximately one minute of execution time for the solution. The MSC/PROBE model required approximately forty minutes of execution time for all p-levels 1-8.

SUMMARY OF RESULTS AND CONCLUSIONS

The COSTAR and MSC/PROBE finite element programs predict almost exactly the same magnitudes of springback for a range of geometries and materials. Less time was required to construct the MSC/PROBE models due to the fewer number of elements. The addition of the orthotropic material angle in MSC/PROBE Version 4.1 further reduces the amount of modeling time required.

A single execution of the COSTAR model was used throughout this project as a comparison to the eight p-levels solutions available with MSC/PROBE. This is an important factor due to the error encountered in the final stiffened skin model. The COSTAR model must be re-meshed in order to improve the solution. The MSC/PROBE model would require less extensive alterations and, therefore, requires less time to improve the solution.

The two programs show good agreement with actual results. A stiffened panel of the same dimensions and material properties as those modeled was previously fabricated and bonded. The total springback measured for the panel was 0.29 inches. The magnitude of the springback predicted by both COSTAR and MSC/PROBE is 0.22 inches for a difference of 24%.

FUTURE WORK

The finite element methods used for this study have been shown

to predict the correct deflected geometry of a thermoplastic stiffened skin. Current research has shown that such factors as material properties and geometry have a great impact on the magnitude of springback in a composite part. Other physical and model parameters should be investigated in order to improve the predicted magnitudes of springback.

The bondline of the stiffened skin was thought to have little effect on springback and was not modeled. This may be an important omission from the model. Material properties, particularly the through thickness CTE, must be accurately determined for use in springback prediction. Thermoset materials experience a chemical shrinkage during cure which effectively increases the through thickness CTE. This effect must be accurately quantified if thermoset springback prediction is to be accomplished.

Geometry plays an important role in springback prediction. Current models require two dimensional representation only. Eventually this must be extended to three dimensions. Plane strain plate elements are used for the two dimensional cases and seem to be the most reliable. Other element formulations may prove to be more accurate. The type of element to be used for the three dimensional case has not been investigated.

The solution used for this project was for an applied load of a single temperature step. Material properties were held constant over the entire interval. The actual case would change the material properties as the part is cooled from the stress free state. A piecewise linear solution may be more realistic than the single interval used for this study. Several temperature steps should be applied to the model with material properties varied accordingly for each interval. This load and material property condition would more realistically model the actual behavior of the part as it cools.

RECOMMENDED APPROACH FOR SPRINGBACK PREDICTIONS

1. Verify all geometry and use on the finite element model as

accurately as possible.

2. Components with three-dimensional curvature should be sectioned into appropriate two-dimensional sections, if at all possible. Solid element modeling of complex three-dimensional parts is possible, but the advantages over 2-D modeling are limited and normally not worth the additional modeling time.
3. Two-dimensional generalized plane strain elements are recommended. These elements seem to most closely model the actual stress/strain behavior of the material, particularly if the material is a composite.
4. At least five elements should be used to define a radius. Four elements through the thickness are necessary for an h-version finite element code while only one element is required for a p-version code.
5. Temperature dependent orthotropic properties should be used to define the materials. The properties should be broken into corresponding temperature intervals, the size of which will depend on the material and overall change in temperature.
6. The finite element model is then run for each of the defined temperature intervals with corresponding material properties. The final solution is the summation of the resulting deflections from each analysis run.

REFERENCES

1. Barnes, J. A., Simms, I. J., et. al., "Thermal Expansion Characteristics of PEEK Composites", Journal of Material Science, June, 1990.
2. Moore, D. R., et. al., "Mechanical Properties for Design and Analysis of Carbon Fibre Reinforced PEEK Composite Structures", Presented at European SAMPE Conference, Birmingham, U. K., July, 1989.
3. Fahmy, A. A. and Ragai-Ellozy, A. N., "Thermal Expansion of Laminated Fiber Composites in the Thickness Direction", Journal of Composite Materials, vol. 8, pp. 90-92, 1974.
4. Zahlan, N., "Design with Thermoplastic Based Composites; Thermal Effect Considerations", Presented at IMECHE on 'Design in Composites', London, U. K., March, 1989.
5. Zahlan, N. and O'Neill, J. M., "Design and Fabrication of Composite Components; the Spring-Forward Phenomenon", Journal of Composite Materials, January, 1989.
6. Jeronimidis, G. and Parkyn, A. T., "Residual Stresses in Carbon Fibre-Thermoplastic Matrix Laminates", University of Reading, U. K., August, 1987.
7. Goering, J., "Composite Structural Analysis Routine User's Manual for Version 4.1", McDonnell Aircraft Company, St. Louis, MO, 1989.
8. Szabo', B. A., and Babuska, I., Finite Element Analysis, John Wiley and Sons, Inc., 1991.
9. Szabo', B. A., "PROBE Theoretical Manual, Release 1.0", Noetic Technologies Corporation, St. Louis, MO, 1985.

10. Fracchia, C. A., "Determination of the Effective Elastic Constants of Thick Laminated Composites (THICKLAM User's Guide)", McDonnell Aircraft Company, AMS Tech Note AMS-TN-90-4, 1991.
11. Jones, R. M., Mechanics of Composite Materials, Hemisphere Publishing Corporation, pp. 147-237, 1975.
12. Sun, C. T., "Three-Dimensional Effective Elastic Constants for Thick Laminates", Journal of Composite Materials, vol. 22, pp. 629-639, 1988.

TABLE 1. DISPLACEMENT RESULTS FOR CASE I, ISOTROPIC MATERIAL

MSC/PROBE			COSTAR		
Node #	Delta X	Delta Y	Node #	Delta X	Delta Y
1	0.0	-0.0200	1	0.0	-0.01999
5	0.0	-0.212	5	0.0	-0.02118
931	-0.0128	-0.00166	437	-0.01288	-0.00156
936	-0.137	-0.00242	141	-0.01378	-0.00234
911	-0.0502	0.0	911	-0.05022	0.0
915	-0.0502	-0.00120	915	-0.05022	-0.00197

GP14-0169-11-D/cm

TABLE 2. ERROR ESTIMATION FOR CASE 1, ISOTROPIC MATERIAL

P	Global DOF	Delta Y	Extrapolated Energy	Convergence Rate	Percent Rel Error Est'd
1	120	0.102792D-01	0.000000D+00	0.00	*****
2	304	0.490144D-05	0.000000D+00	9.65	60.25
3	488	0.431920D-05	0.431515D-05	1.25	44.84
4	736	0.408346D-05	0.385223D-05	0.96	36.81
5	1048	0.401905D-05	0.398416D-05	0.40	34.29
6	1424	0.381051D-05	0.356409D-05	2.22	24.41
7	1864	0.377486D-05	0.376470D-05	0.68	22.29
8	2368	0.370690D-05	0.359619D-05	2.00	17.55

GP14-0169-12-D/cm

**ORIGINAL PAGE IS
OF POOR QUALITY**

TABLE 3. DISPLACEMENT RESULTS FOR CASE II, ORTHOTROPIC MATERIAL

MSC/PROBE			COSTAR		
Node #	Delta X	Delta Y	Node #	Delta X	Delta Y
1	0.0	0.00371	1	0.0	0.00372
5	0.0	0.00300	5	0.0	-0.00301
931	-0.0143	0.00082	437	-0.01443	-0.00078
936	-0.0144	-0.00010	441	-0.01457	-0.00012
911	-0.0152	0.0	911	-0.01533	0.0
915	-0.0152	-0.00071	915	-0.01533	-0.00071

GP14-0169-13-D/cm

**TABLE 4. DISPLACEMENT RESULTS FOR
CASE III, ORTHOTROPIC MATERIAL,
REVISED MSC/PROBE MESH**

MSC/PROBE		
Node #	Delta X	Delta Y
1	0.0	0.00372
5	0.0	0.00301
931	-0.0148	0.00034
936	-0.0148	-0.00045
911	-0.0153	0.0
915	-0.0153	-0.00071

GP14-0169-14-D/cm

TABLE 5. ERROR ESTIMATION FOR CASE III, REVISED MSC/PROBE MODEL, ORTHOTROPIC MATERIAL

P	Global DOF	Total Energy	Extrapolated Energy	Convergence Rate	Percent Rel Error Est'd
1	152	0.682723D-02	0.000000D+00	0.00	*****
2	348	0.407940D-05	0.000000D+00	9.82	47.89
3	616	0.391884D-05	0.391814D-05	0.50	42.54
4	928	0.370865D-05	0.354308D-05	1.05	34.29
5	1320	0.355625D-05	0.266208D-05	1.41	26.77
6	1792	0.344546D-05	0.282333D-05	2.05	19.57
7	2344	0.338463D-05	0.327377D-05	2.43	14.12
8	2976	0.335552D-05	0.331843D-05	2.43	10.57

GP14-0169-15-D/rr

TABLE 6a. MATERIAL PROPERTY CALCULATIONS FOR THE CORRUGATION

THICKLAM assumes that the composite is a balanced, symmetric laminate of one material system.

Input

Material System	IM7/PEEK
Lamina Orientation	
Angle 1	0°
Angle 2	45°
Angle 3	-45°
Angle 4	90°
Angle 5	
Angle 6	
Angle 7	
Angle 8	
Lamina Data	
E ₁	2.24E+07
E ₂	1.30E+06
E ₃	1.30E+06
μ ₁₂	0.350
μ ₁₃	0.020
μ ₂₃	0.480
G ₁₂	7.90E+05
G ₁₃	7.90E+05
G ₂₃	4.50E+05
μ ₂₁	0.020
μ ₃₁	0.001
μ ₃₂	0.480
Δ	2.01308E-20

Temperature	RT
Moisture Content	Dry
Percent Thickness	
Angle 1	30.9%
Angle 2	30.8%
Angle 3	30.8%
Angle 4	7.7%
Angle 5	
Angle 6	
Angle 7	
Angle 8	
Total Thickness	0.07

Output

Lamina (C) Matrix	
C11	2.26E+07
C12	6.14E+05
C13	3.21E+05
C22	1.71E+06
C23	8.20E+05
C33	1.69E+06
C44	4.50E+05
C55	7.90E+05
C66	7.90E+05
Laminate Data	
E _x (E ₃)	9.46E+06
E _y (E ₁)	5.38E+06
E _z (E ₂)	1.63E+06
μ _{xy} (μ ₃₁)	0.541
μ _{xz} (μ ₃₂)	0.102
μ _{yz} (μ ₁₂)	0.278
G _{xy} (G ₃₁)	3.86E+06
G _{xz} (G ₃₂)	6.12E+05
G _{yz} (G ₁₂)	5.39E+05
μ _{yx} (μ ₁₃)	0.307
μ _{zx} (μ ₂₃)	0.018
μ _{zy} (μ ₂₁)	0.084

GP14-0169-16-D/rr

TABLE 6b. MATERIAL PROPERTY CALCULATIONS FOR THE FLAT SKIN PANEL

THICKLAM assumes that the composite is a balanced, symmetric laminate of one material system.

Input

Material System	IM7/PEEK
Lamina Orientation	
Angle 1	0°
Angle 2	45°
Angle 3	-45°
Angle 4	90°
Angle 5	
Angle 6	
Angle 7	
Angle 8	
Lamina Data	
E ₁	2.24E+07
E ₂	1.30E+06
E ₃	1.30E+06
μ ₁₂	0.350
μ ₁₃	0.020
μ ₂₃	0.480
G ₁₂	7.90E+05
G ₁₃	7.90E+05
G ₂₃	4.50E+05
μ ₂₁	0.020
μ ₃₁	0.001
μ ₃₂	0.480
Δ	2.01308E-20

Temperature	RT
Moisture Content	Dry
Percent Thickness	
Angle 1	30.9%
Angle 2	30.8%
Angle 3	30.8%
Angle 4	7.7%
Angle 5	
Angle 6	
Angle 7	
Angle 8	
Total Thickness	0.07

Output

Lamina (C) Matrix	
C11	2.26E+07
C12	6.14E+05
C13	3.21E+05
C22	1.71E+06
C23	8.20E+05
C33	1.69E+06
C44	4.50E+05
C55	7.90E+05
C66	7.90E+05
Laminate Data	
E _x (E ₃)	1.14E+07
E _y (E ₁)	7.37E+06
E _z (E ₂)	1.64E+06
μ _{xy} (μ ₃₁)	0.308
μ _{xz} (μ ₃₂)	0.194
μ _{yz} (μ ₁₂)	0.305
G _{xy} (G ₃₁)	2.78E+06
G _{xz} (G ₃₂)	6.07E+05
G _{yz} (G ₁₂)	5.44E+05
μ _{yx} (μ ₁₃)	0.200
μ _{zx} (μ ₂₃)	0.028
μ _{zy} (μ ₂₁)	0.068

GP14-0169-17-D/rr

TABLE 7. DISPLACEMENT RESULTS FOR THE FULL STIFFENED SKIN

MSC/PROBE			COSTAR		
Node #	Delta X	Delta Y	Node #	Delta X	Delta Y
236	-0.00952	0.0949	1	-0.00728	0.10900
229	-0.01100	0.0940	11	-0.01196	0.10660
363	-0.00580	0.0616	103	-0.00564	0.06158
237	-0.00793	0.0603	116	-0.00637	0.05993

GP14-0169-18-D/cm

TABLE 8. ERROR ESTIMATION FOR THE HAT-STIFFENED SKIN

P	Global DOF	Total Energy	Extrapolated Energy	Convergence Rate	Percent Rel Error Est'd
4	3467	0.171003D+00	0.000000D+00	0.00	14.28
5	4947	0.169596D+00	0.000000D+00	1.49	10.95
6	6733	0.168854D+00	0.167585D+00	1.49	8.70

GP14-0169-19-D/rr

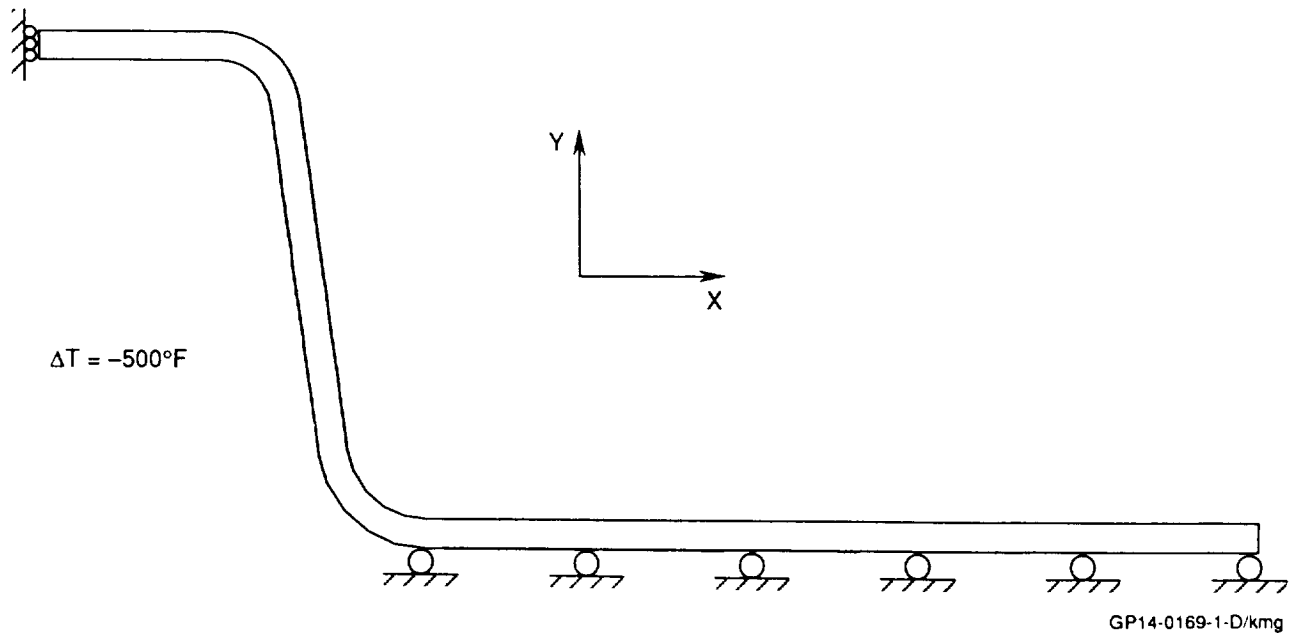


Figure 1. Simple Geometry Model for Baseline Cases I, II, and III

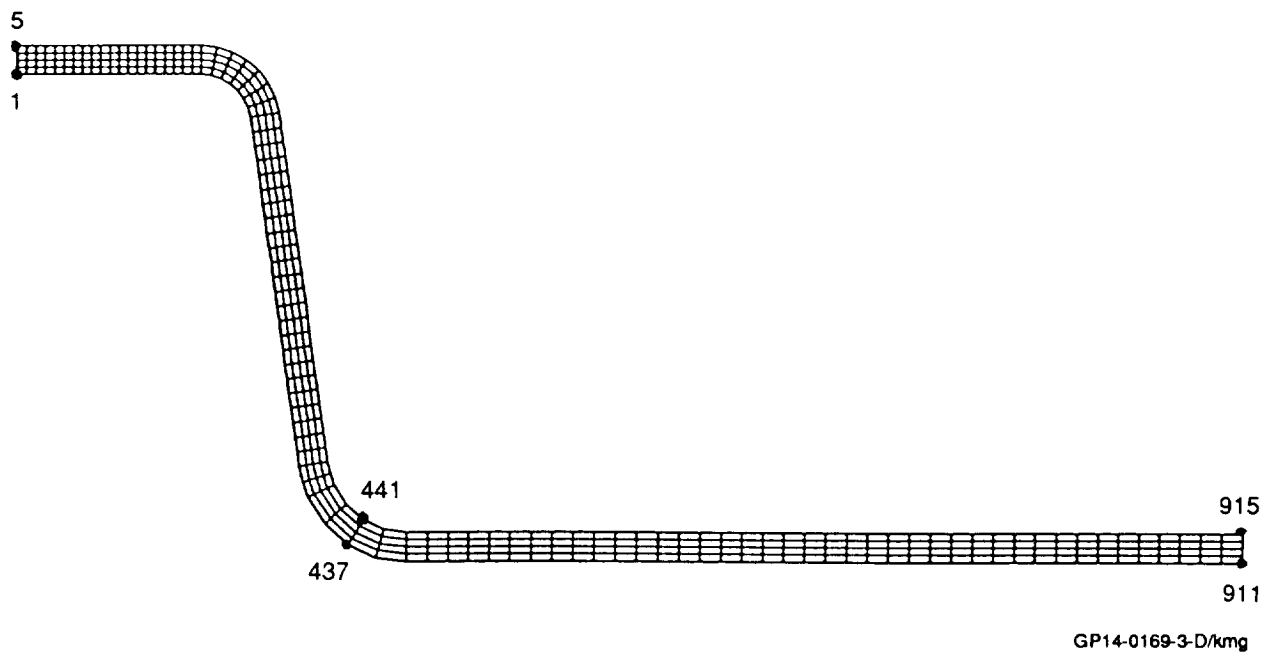


Figure 2a. Simple Geometry, COSTAR Model Discretization

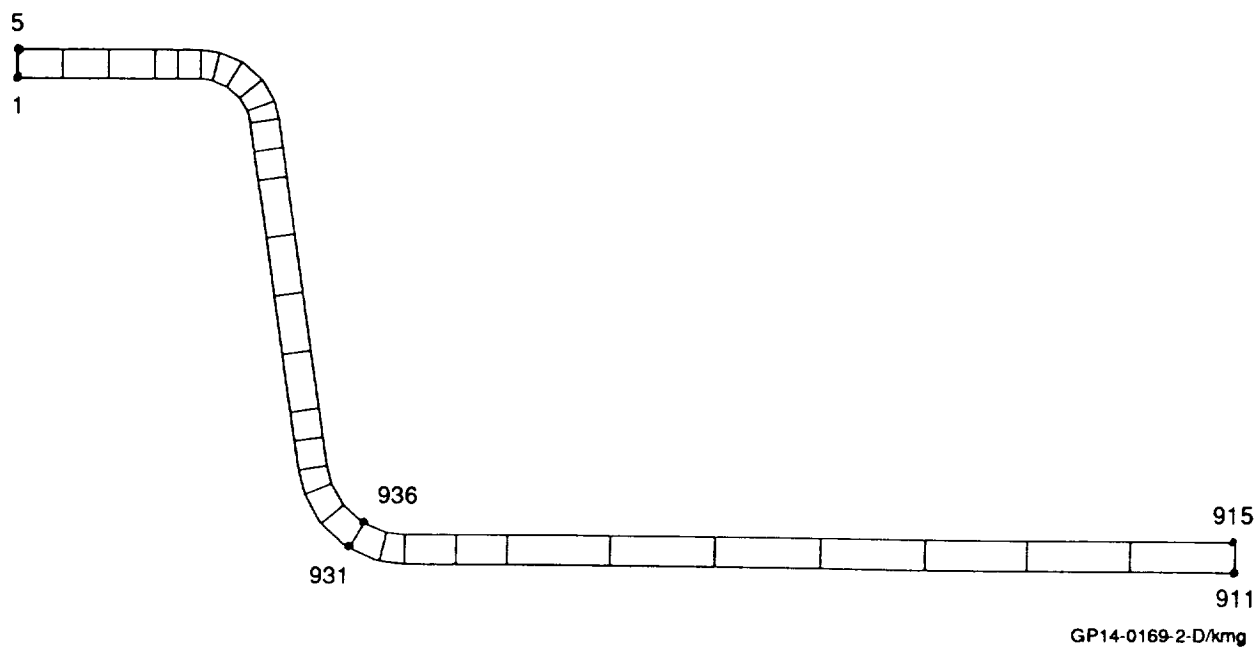


Figure 2b. Simple Geometry, MSC/PROBE Model Discretization

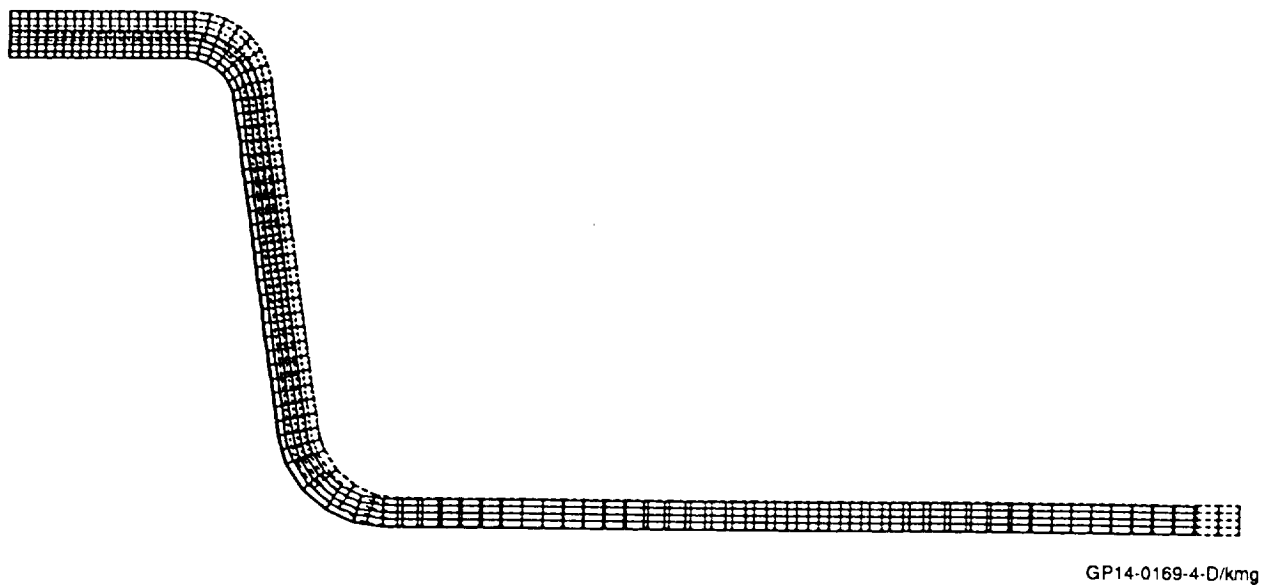
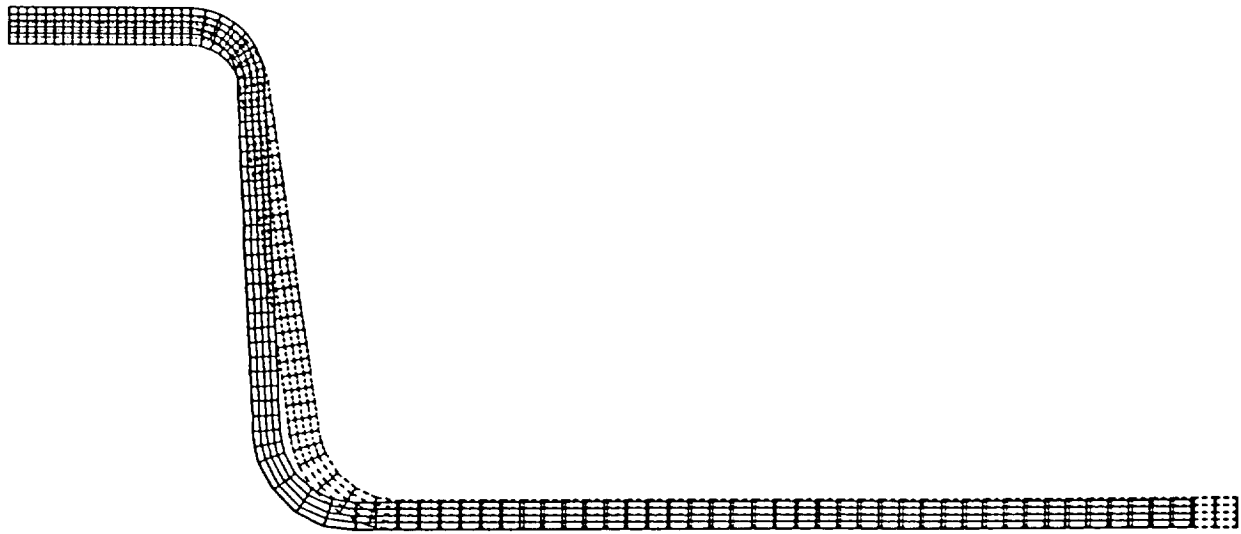
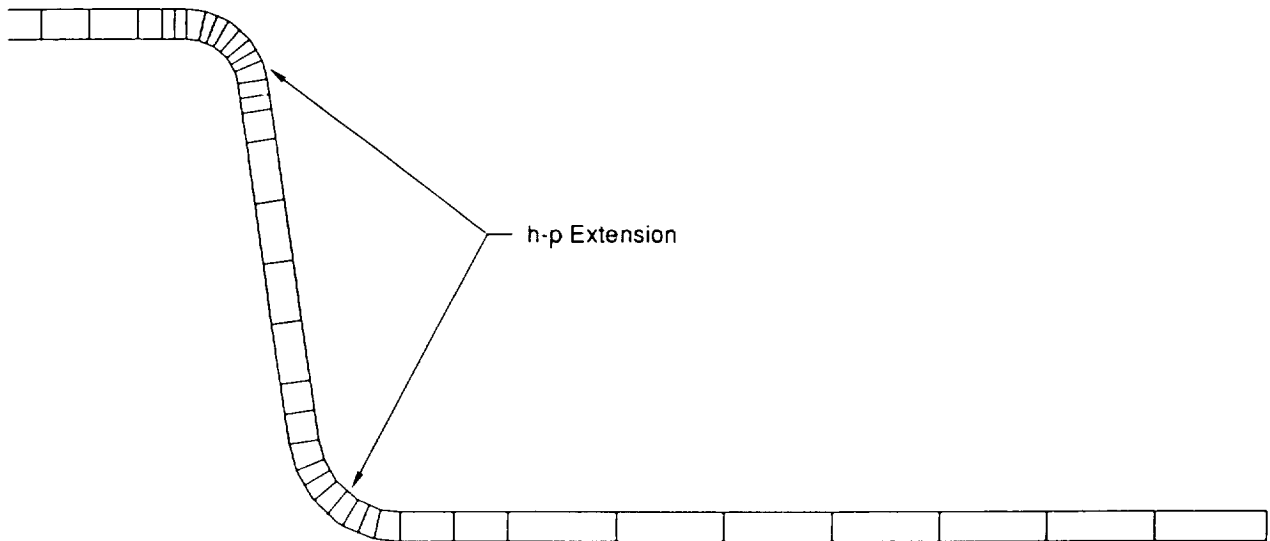


Figure 3. Deflected Geometry for Case I Isotropic Material



GP14-0169-5-D/kmg

Figure 4. Deflected Geometry for Case II, Orthotropic Material



GP14-0169-6-D/kmg

Figure 5. MSC/PROBE Model for Case III, Refined Mesh

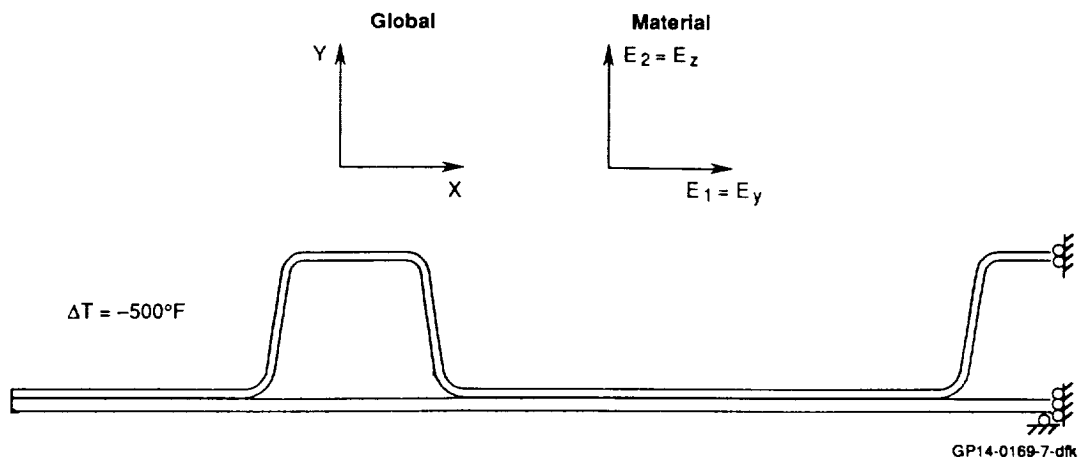


Figure 6. Geometry for the Full Hat-Stiffened Skin

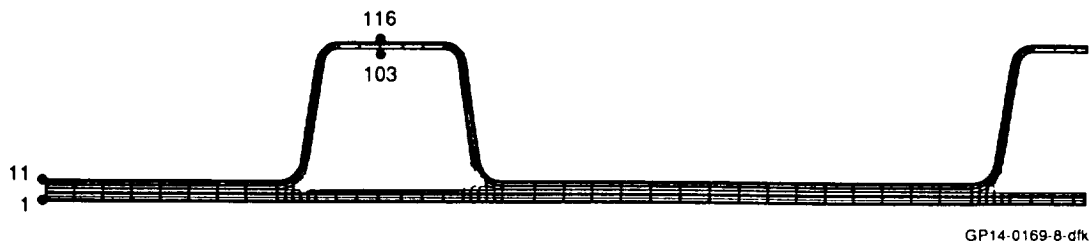


Figure 7a. COSTAR Model for the Hat-Stiffened Skin

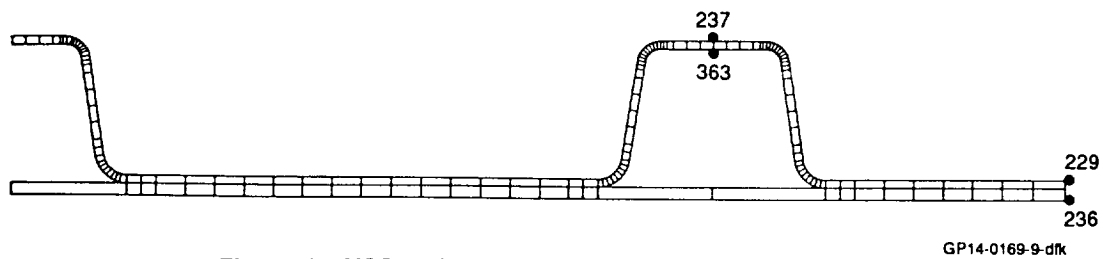


Figure 7b. MSC/PROBE Model for the Hat-Stiffened Skin

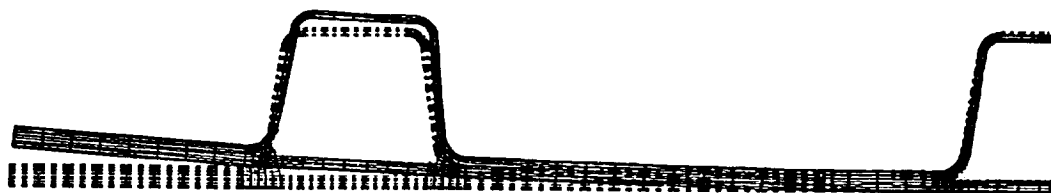


Figure 8. Deflected Geometry for the Hat-Stiffened Skin

SESSION XI
SPACE STRUCTURES

THIS PAGE INTENTIONALLY BLANK